

## Bryn Mawr College Scholarship, Research, and Creative Work at Bryn Mawr College

Physics Faculty Research and Scholarship

Physics

2016

# Observations of High Vibrational Levels of the $4f\sigma$ $41\Sigma^+$ u State of $H_2$

Alexander M. Chartrand

Bryn Mawr College, [achartrand@brynmawr.edu](mailto:achartrand@brynmawr.edu)

Robert C. Ekey Jr.

University of Mount Union, [ekeyrc@mountunion.edu](mailto:ekeyrc@mountunion.edu)

Elizabeth F. McCormack

Bryn Mawr College, [emccorma@brynmawr.edu](mailto:emccorma@brynmawr.edu)

[Let us know how access to this document benefits you.](#)

Follow this and additional works at: [http://repository.brynmawr.edu/physics\\_pubs](http://repository.brynmawr.edu/physics_pubs)



Part of the [Atomic, Molecular and Optical Physics Commons](#)

### Custom Citation

Alexander Chartrand, Robert Ekey, Jr., Elizabeth McCormack, "Observations of High Vibrational Levels of the  $4f\sigma$   $41\Sigma^+$  u State of  $H_2$ ," *The Journal of Chemical Physics*, 145, 024306 (2016), DOI:<http://dx.doi.org/10.1063/1.4955197>.

This paper is posted at Scholarship, Research, and Creative Work at Bryn Mawr College. [http://repository.brynmawr.edu/physics\\_pubs/94](http://repository.brynmawr.edu/physics_pubs/94)

For more information, please contact [repository@brynmawr.edu](mailto:repository@brynmawr.edu).

## Observations of high vibrational levels of the $4f\sigma 41\Sigma^+$ state of $H_2$

A. M. Chartrand, R. C. Ekey, and E. F. McCormack

Citation: *The Journal of Chemical Physics* **145**, 024306 (2016); doi: 10.1063/1.4955197

View online: <http://dx.doi.org/10.1063/1.4955197>

View Table of Contents: <http://scitation.aip.org/content/aip/journal/jcp/145/2?ver=pdfcov>

Published by the AIP Publishing

### Articles you may be interested in

Observations of the high vibrational levels of the  $B''B\ 1\Sigma^+$  state of  $H_2$

*J. Chem. Phys.* **144**, 014307 (2016); 10.1063/1.4939079

Coherent superposition of M-states in a single rovibrational level of  $H_2$  by Stark-induced adiabatic Raman passage

*J. Chem. Phys.* **140**, 074201 (2014); 10.1063/1.4865131

Spectral identification of diffuse resonances in  $H_2$  above the  $n = 2$  dissociation limit

*J. Chem. Phys.* **134**, 054309 (2011); 10.1063/1.3544300

Quasiclassical trajectory calculations for  $Li(22PJ) + H_2 \rightarrow LiH(X1\Sigma^+) + H$ : Influence by vibrational excitation and translational energy

*J. Chem. Phys.* **134**, 034119 (2011); 10.1063/1.3519801

$(2 + 1)$  Resonance-enhanced ionization spectroscopy of a state-selected beam of OH radicals

*J. Chem. Phys.* **123**, 074309 (2005); 10.1063/1.1997132



# NEW Special Topic Sections

**NOW ONLINE**  
Lithium Niobate Properties and Applications:  
Reviews of Emerging Trends

**AIP** Applied Physics Reviews

# Observations of high vibrational levels of the $4f\sigma$ $4^1\Sigma_u^+$ state of $H_2$

A. M. Chartrand,<sup>1,a)</sup> R. C. Ekey,<sup>2</sup> and E. F. McCormack<sup>1</sup>

<sup>1</sup>Department of Physics, Bryn Mawr College, Bryn Mawr, Pennsylvania 19010, USA

<sup>2</sup>Physics and Astronomy Department, University of Mount Union, Alliance, Ohio 44601, USA

(Received 19 May 2016; accepted 21 June 2016; published online 12 July 2016)

Resonantly enhanced multiphoton ionization via the  $EF^1\Sigma_g^+$ ,  $v' = 6$  double-well state has been used to probe the energy region below the third dissociation limit of  $H_2$  where several high vibrational levels of the  $4^1\Sigma_u^+$  state are expected. Theoretical *ab initio* potential energy curves for this state predict a deep inner well and shallow outer well where vibrational levels above  $v = 8$  are expected to exhibit the double-well character of the state. Since the  $4^1\Sigma_u^+$  state has  $f$ -state character, transitions to it from the ground state are nominally forbidden. However, the  $d$  character of the outer well of the  $EF^1\Sigma_g^+$  state allows access to this state. We report observations of transitions to the  $v = 9$ – $12$  levels of the  $4^1\Sigma_u^+$  state and compare their energies to predicted energies calculated from an *ab initio* potential energy curve with adiabatic corrections. Assignments are based on measured energies and linewidths, rotational constants, and expected transition strengths. The amount of agreement between the predicted values and the observations is mixed, with the largest discrepancies arising for the  $v = 9$  level, owing to strong nonadiabatic electronic mixing in this energy region. *Published by AIP Publishing*. [<http://dx.doi.org/10.1063/1.4955197>]

## I. INTRODUCTION

The  $4f\sigma$   $4^1\Sigma_u^+$  state is the fourth in a series of *ungerade* sigma states of the hydrogen molecule. As shown in Fig. 1, this state has a double-well structure caused by an avoided crossing with the  $(2s\sigma, 2p\sigma)$  doubly excited state at an internuclear distance around  $5 a_0$  and another avoided crossing with the  $4p\sigma B''\bar{B}^1\Sigma_u^+$  curve at around  $5.7 a_0$ . At small internuclear separations, this state has  $(1s\sigma, 4f\sigma)$  character, for which one-photon transitions from the  $(1s\sigma)^2$  ground state are nominally forbidden. The  $V^1\Pi_u$  state which has  $(1s\sigma, 4f\pi)$  character is also shown. Note how for low vibrational levels, the  $4f\sigma$  and the  $4f\pi$  curves are nearly degenerate, whereas at larger  $R$ , and therefore higher vibrational levels, we expect to see clear differences in their rovibrational structures.

Levels belonging to the  $4f$  manifold of states have been identified previously in infrared emission corresponding to low- $v$   $5g$ – $4f$  and  $4f$ – $3d$  transitions.<sup>4,5</sup> Only very recently have a number of unidentified ground state absorption features been attributed to transitions to low- $v$   $f$ -states, which appear through weak  $p \sim f$  partial wave mixing.<sup>4,6,7</sup> The current experiment takes advantage of the mixed electronic character of the outer well of the  $EF^1\Sigma_g^+$  state, produced by an avoided crossing with the doubly excited  $(2p\sigma)^2$  state.<sup>8</sup> As a result, the vibrational levels have mixed  $s$ , doubly excited  $p$ , and  $d$  character.<sup>9</sup> The mixing for the  $v' = 6$  level of the  $EF^1\Sigma_g^+$  state is  $\sim 75\%$   $s$ ,  $25\%$  doubly excited  $p$  and singly excited  $d$  character. The  $d$  character allows access to the  $4f\sigma 4^1\Sigma_u^+$  state via state-selective single-photon excitation resulting in strong spectral features that allow an in-depth rovibrational analysis.

Staszewska and Wolniewicz<sup>1</sup> have predicted the  $v = 0$ – $14$ ,  $J = 0$  energies and rotational constants,  $B_v$ , for

the  $4^1\Sigma_u^+$  state using an *ab initio* potential energy curve with adiabatic corrections. Calculations of the nonadiabatic couplings between the lowest six  $^1\Sigma_u^+$  and lowest four  $^1\Pi_u$  states of  $H_2$  have also been made by Wolniewicz, Orlikowski, and Staszewska<sup>10</sup> and used to calculate an accurate energy for the  $v = 8$ ,  $J = 0$  level of the  $4^1\Sigma_u^+$  state to correct a misassignment made in an earlier experimental study.<sup>11</sup> The non-adiabatic coupling between the  $v = 8$ ,  $J = 0$  level and the  $v = 50$ ,  $J = 0$  level of the  $B''\bar{B}^1\Sigma_u^+$  state is one of many examples of strong mixing between high- $v$  levels of the  $4^1\Sigma_u^+$ , the  $B''\bar{B}^1\Sigma_u^+$ , and the  $V^1\Pi_u$  states, making the spectra in this energy region very complex. While the non-adiabatic couplings have been computed and their effects on the energy levels of the  $B''\bar{B}^1\Sigma_u^+$  state have been reported, such adjusted energies for levels of the  $4^1\Sigma_u^+$ , and the  $V^1\Pi_u$  state have not yet been reported, presumably due to the challenges presented by the calculations.

Recently we completed a study of the  $B''\bar{B}^1\Sigma_u^+$  state using resonantly enhanced multiphoton ionization via the  $EF^1\Sigma_g^+$ ,  $v' = 6$  double-well state. This was published in three segments: low vibrational, predominately outer-well  $\bar{B}$  states,<sup>11</sup> states near the third dissociation threshold,<sup>12</sup> and states in the energy region in between.<sup>13</sup> The higher vibrational assignments were aided significantly by the non-adiabatic calculations of the  $B''\bar{B}^1\Sigma_u^+$  state by Wolniewicz, Orlikowski, and Staszewska<sup>10</sup> and the recent works on  $p$ -character valence states and electronic Rydberg states of  $H_2$  by Glass-Maujean *et al.*<sup>14–18</sup>

Here, we address the assignment of several observed transitions not assigned in our previous studies. The nonadiabatic calculations by Wolniewicz, Orlikowski, and Staszewska<sup>10</sup> predict strong mixing between the high vibrational levels of the  $B''\bar{B}^1\Sigma_u^+$  state and the  $4^1\Sigma_u^+$  state. This, in addition to the ability to access  $f$ -character states

<sup>a)</sup>achartrand@brynmaur.edu

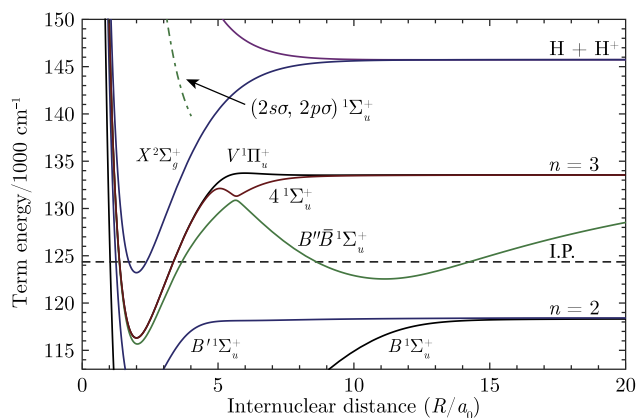


FIG. 1. *Ab initio* potential energy curves of the four lowest  $1\Sigma_u^+$  states (Ref. 1) and the  $V^1\Pi_u$  state (Ref. 2) of  $H_2$ . The dashed line indicates the ionization potential of the molecule, while the green dotted-dashed line is the doubly excited  $(2s\sigma, 2p\sigma)$  state (Ref. 3).

from the  $EF^1\Sigma_g^+$  state,<sup>9,19</sup> led us to consider assignments to levels of the  $4^1\Sigma_u^+$  state. Specific assignments have been guided by  $\Sigma-\Sigma$  transition patterns, observed energies, rotational dependencies, and relative transition strengths. We report measured term energies, rotational constants, and linewidths for the  $v = 9-12$  levels of the  $4^1\Sigma_u^+$  state and compare them to the theoretical results of Staszewska and Wolniewicz.<sup>1</sup>

## II. EXPERIMENT

The experimental setup has been described previously in detail.<sup>13,20</sup> Briefly, double resonance spectroscopy via the  $J' = 0-2$  rotational levels of the  $EF^1\Sigma_g^+$ ,  $v' = 6$  state was used to probe the energy region between 131 100 and 133 700  $\text{cm}^{-1}$  above the  $X^1\Sigma_g^+$ ,  $v'' = 0$ ,  $J'' = 0$  ground state of  $H_2$ . Two pulsed Nd:YAG-pumped dye lasers and a vacuum chamber housing a pulsed-valve molecular beam source and a time of flight mass spectrometer were used to obtain double-resonance ionization spectra. Pump light with a wavelength near 193 nm is used to excite the  $EF^1\Sigma_g^+$ ,  $v' = 6$ ,  $J' = 0-2 \leftarrow X^1\Sigma_g^+$ ,  $v'' = 0$ ,  $J'' = 0-2$  two-photon transitions. This light was generated by sum-frequency mixing in a beta barium borate crystal (BBO) the fourth harmonic of Nd:YAG laser light at 266 nm with the output of a pumped dye laser operated at  $\sim 705$  nm. Probe laser output at 663–725 nm from the second dye laser was frequency doubled in a BBO and then used to excite single photon transitions from the  $EF^1\Sigma_g^+$  state to the states of interest as depicted in Fig. 2.

A collision-free beam of molecular hydrogen was produced by using a supersonic expansion of pure  $H_2$  from a solenoid-driven pulsed valve. Counter-propagating pump and probe light pulses crossed the molecular beam in an interaction region located between two electric field plates. The pump light pulses were typically on the order of 30  $\mu\text{J}$  and focused into the chamber with a 50-cm lens. Probe light pulses were focused into the chamber with a 30-cm lens to a spot size of  $\sim 100$   $\mu\text{m}$ . Ions generated by the two-color process were accelerated into the time of flight mass spectrometer by a pulsed electric field of 125 V/cm applied across the plates. A time delay of 40 ns was introduced between the pump

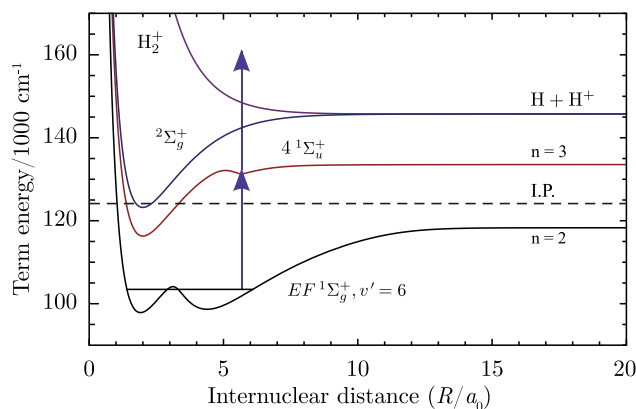


FIG. 2. Probe excitation scheme and generation of  $H^+$  ions.

and probe laser pulses to distinguish ions produced by the pump beam alone, and those produced by two-color resonant excitation. Spectra are produced by scanning the frequency of the probe light while monitoring the production of  $H^+$  ions by using a boxcar integrator with a timed gate set to collect the ions.

Energies and linewidths for transitions were extracted by making Beutler-Fano profile fits to the observed peaks. The behavior of the linewidth as a function of the probe laser intensity was used to find an equivalent zero-intensity linewidth by linear extrapolation. The optogalvanic effect in argon provides reference transitions at known energies and an etalon provides an independent measure of the linearity of the wavelength scans in the predoubled probe laser output. Both are used to provide calibrated probe laser wavelengths. The energy uncertainties reported in Sec. III are standard deviations observed from data taken from multiple scans. These reflect the energy uncertainty of the doubled light associated with the calibration peaks ( $\sim 0.02$   $\text{cm}^{-1}$ ), the statistical uncertainties of peak fit to the spectral features ( $\sim 0.2-1$   $\text{cm}^{-1}$ , depending on linewidth), and remaining scan nonlinearities in the spectra ( $\sim 0.1$   $\text{cm}^{-1}$ ). Reported total energies are referenced to the  $X^1\Sigma_g^+$ ,  $v'' = 0$ ,  $J'' = 0$  ground state by using the known  $EF^1\Sigma_g^+$ ,  $v' = 6$  transition energies.<sup>8</sup>

## III. RESULTS AND DISCUSSION

Figs. 3–6 show energy regions associated with proposed assignments to the  $v = 9-12$ ,  $J = 0-3$  levels of the  $4^1\Sigma_u^+$  state. Fig. 3 in particular clearly illustrates a rotational pattern typical of  $\Sigma-\Sigma$  transitions in Hund's case b. In the  $J' = 1$  and 2 pump transition spectra, P and R branches are present, and Q transitions are absent. In addition, the  $J = 1$  level is seen in both the  $J' = 0$  and 2 spectra as an R(0) and P(2) transition at the same term energy. This confirms that the upper level in the transition has dominant  $1\Sigma_u^+$  character. A similar pattern is seen in Figs. 4–6 along with additional transitions. We note that at short range and low  $v$  the  $4f\sigma$  manifold is well described as a molecular Rydberg state in Hund's case d,<sup>4,5</sup> where the possible case b character of an  $f$  state –  $\Sigma$ ,  $\Pi$ ,  $\Delta$ , and  $\Phi$  – is nominally mixed. For the high

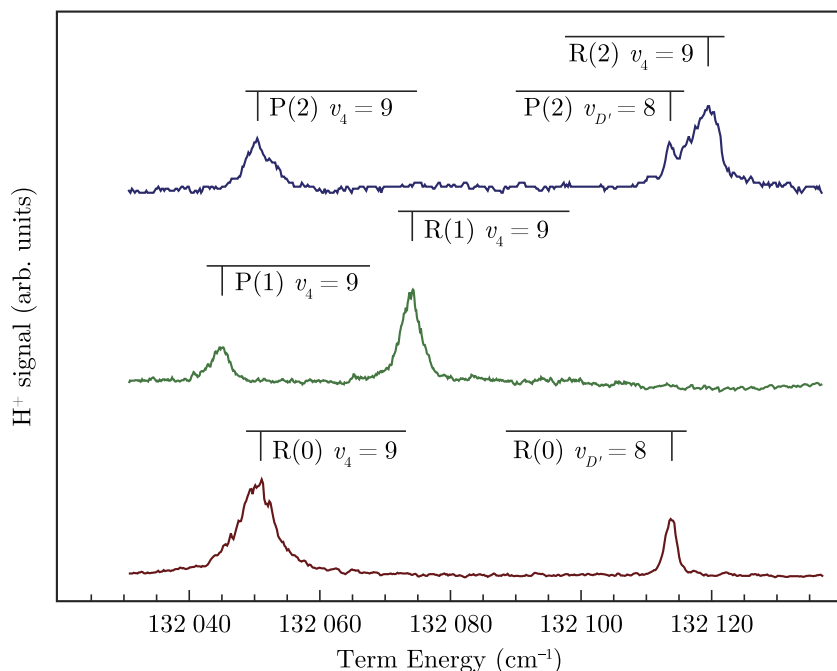


FIG. 3. Spectra showing the  $4^1\Sigma_u^+, v=9$  state. From bottom to top are the spectra excited via the  $J'=0$  (red),  $J'=1$  (green), and  $J'=2$  (blue)  $EF^1\Sigma_g^+, v'=6$  level. Additional assignments in this region are to the  $D'^1\Pi_u^+$  state.<sup>21</sup>

vibrational levels considered here, the observed  $\Sigma$ – $\Sigma$  pattern indicates that the  $\Sigma$  component dominates over the  $\Pi$ ,  $\Delta$ , and  $\Phi$  components.

In Table I, the experimental term energies and rotational constants are compared to values obtained from the *ab initio* potential energy curve with adiabatic corrections calculated by Staszewska and Wolniewicz.<sup>1</sup> They noted that the adiabatic energies they reported for the  $4^1\Sigma_u^+$  state may be less reliable due to potentially larger nonadiabatic corrections. With this in mind, the experimental rotational constants and vibrational energies are in reasonable agreement, with the exception, however, of the  $v=9$  levels.

Fig. 7 compares the energies and wavefunctions of the  $v=9$  level obtained from the *ab initio* Born-Oppenheimer and

adiabatic potential energy curves. In both cases the probability of the  $v=9$  level residing in the small outer well is 83%–90%, and it corresponds to the vibrational ground state of the outer well. Since the minimum of this well coincides with the avoided crossing of the  $4^1\Sigma_u^+$  state with the  $B''\bar{B}^1\Sigma_u^+$  state, calculations of the  $v=9$  energy and wavefunction are strongly affected by the adiabatic corrections. As shown, it shifts the calculated energy up by  $\sim 400$   $\text{cm}^{-1}$ . The measured  $v=9$  energy given in Table I falls between the two theoretical values. In addition to the adiabatic effects, nonadiabatic electronic mixing with the  $v=53$  level of the  $B''\bar{B}^1\Sigma_u^+$  state is calculated<sup>10</sup> to be  $\sim 20\%$ , which will also affect the  $v=9$  energy. Taking these into account, the observed level of discrepancy is not unreasonable.

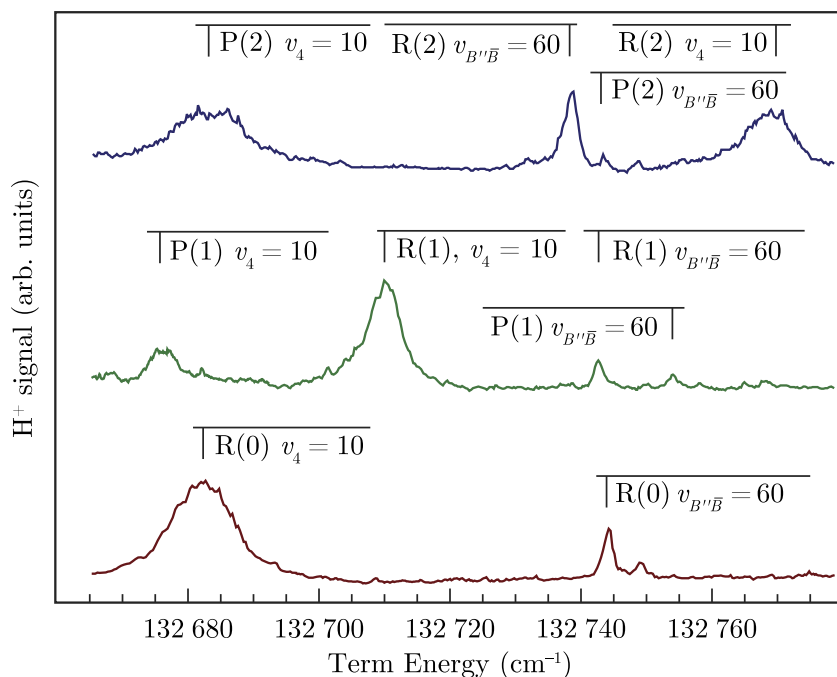


FIG. 4. Spectra showing the  $4^1\Sigma_u^+, v=10$  state. From bottom to top are the spectra excited via the  $J'=0$  (red),  $J'=1$  (green), and  $J'=2$  (blue)  $EF^1\Sigma_g^+, v'=6$  level. Additional assignments in this region are to the  $B''\bar{B}^1\Sigma_u^+$  state.<sup>13</sup>

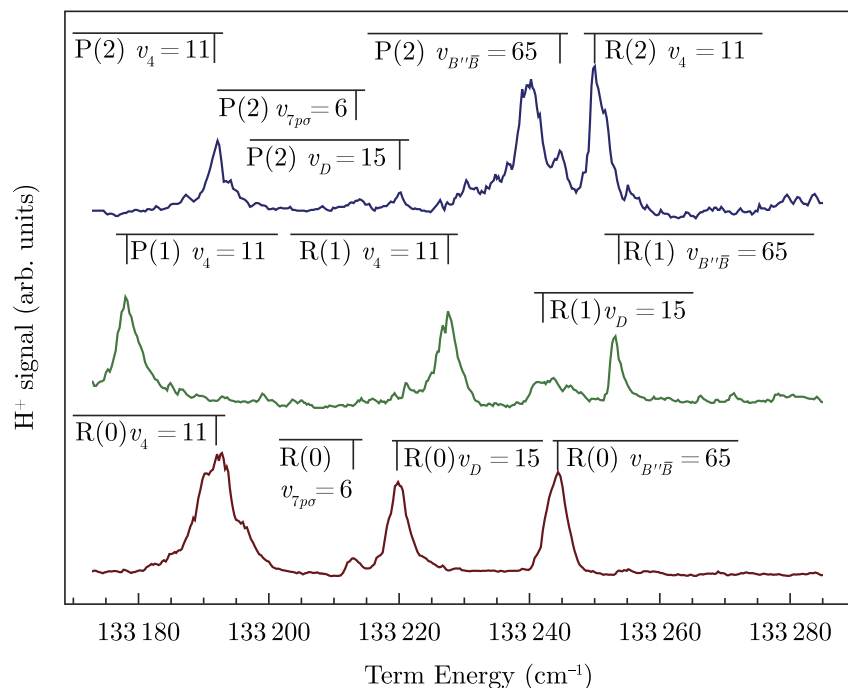


FIG. 5. Spectra showing the  $4^1\Sigma_u^+, v = 11$  state. From bottom to top are the spectra excited via the  $J' = 0$  (red),  $J' = 1$  (green), and  $J' = 2$  (blue)  $EF^1\Sigma_g^+, v' = 6$  level. Additional assignments in this region are to the  $B''\bar{B}^1\Sigma_u^+$ ,  $D'^1\Pi_u^+$  and  $7p\sigma^1\Sigma_u^+$  states (Refs. 13, 22, and 16, respectively).

The term energies for the  $v = 10$  and  $11$  levels are in good agreement with the theory. As reported previously,<sup>13</sup> the  $v = 10$ ,  $J = 3$  level perturbs the  $v = 60$ ,  $J = 3$  level of the  $B''\bar{B}^1\Sigma_u^+$  state. Furthermore, the  $v = 11$ ,  $J = 3$  level interacts with the  $B''\bar{B}^1\Sigma_u^+, v = 65$ ,  $J = 3$  level which explains the unique negative deviation with theory for the  $J = 3$  level in Table I. The  $v = 12$  rotational constant matches that of the adiabatic calculation within 10%. Term energies for the  $v = 12$  level were previously reported in Table 3 of Ref. 12 as unassigned transitions.

In Table I, the  $v = 8$ ,  $J = 0$  experimental energy is compared to both the adiabatic treatment with and without

nonadiabatic corrections.<sup>1,10</sup> The agreement is significantly improved, highlighting the necessity of a full nonadiabatic treatment to predict accurate energies in this complex energy region. Transitions to higher  $J$  values of the  $v = 8$  level consistent with the predicted rotational constant were not observed, and therefore we offer no further assignments to  $v = 8$ .

In previous work<sup>12</sup> we proposed an assignment to the  $v = 13$ ,  $J = 1$  level which was in good agreement with the adiabatic theoretical energy prediction. However, in light of the current observed theoretical and experimental discrepancies, assignments to levels of the  $v = 13$  and  $14$  of

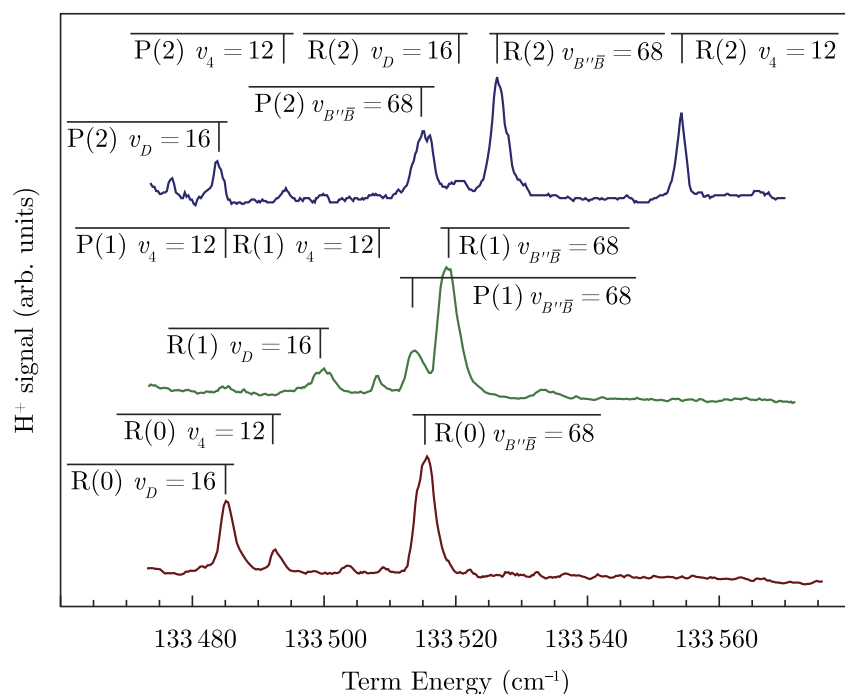


FIG. 6. Spectra showing the  $4^1\Sigma_u^+, v = 12$  state. From bottom to top are the spectra excited via the  $J' = 0$  (red),  $J' = 1$  (green), and  $J' = 2$  (blue)  $EF^1\Sigma_g^+, v' = 6$  level. Additional assignments in this region are to the  $B''\bar{B}^1\Sigma_u^+$  and  $D'^1\Pi_u^+$  states (Refs. 13 and 22, respectively).



TABLE I.  $4^1\Sigma_u^+$  state term energies, rotational constants  $B_v$ , and linewidths  $\Gamma$  in  $\text{cm}^{-1}$ .  $\Delta_E$  and  $\Delta_B$  denote the difference between current observed values and previous calculated values of energy and rotational constant, respectively. (Ref. 1 unless otherwise specified). Uncertainties are noted in parentheses.

$v$	$J$	Term energy	$\Delta_E$	$B_v$	$\Delta_B$	$\Gamma$
8	0	131 613.1(2)	-16.5 +1.4 <sup>a</sup>			
9	0	132 044.3(5)	-367.2	6.8(4)	+1.3	1.9(2)
	1	132 050.9(4)	-371.6			
	2	132 074.9(2)	-369.8			
	3	132 119.7(2)	-358.3			
10	0	132 675.6(3)	-3.3	7.8(5)	-1.9	2.2(5)
	1	132 682.2(9)	-16.3			
	2	132 710.5(7)	-26.6			
	3	132 769.4(5)	-25.9			
11	0	133 178.3(2)	+11.9	6.5(6)	-1.2	1.5(6)
	1	133 191.6(6)	+9.7			
	2	133 227.4(3)	+14.7			
	3	133 250.3(4)	-8.7			
12	0	133 485.4(3)	+59.3	5.5(5)	+0.4	
	1	133 493.4(4)	+57.1			
	2	133 508.4(4)	+51.7			
	3	133 553.9(4)	+66.5			

<sup>a</sup>Table 16 of Ref. 10, nonadiabatic correction applied.

the  $4^1\Sigma_u^+$  state are difficult to make with confidence in this congested energy region.

Fig. 8 compares calculated and measured transition strengths between the  $EF^1\Sigma_g^+$ ,  $v' = 6$  and the  $4^1\Sigma_u^+$ ,  $v = 9$ –12 vibrational levels. *Ab initio* electronic transition moments published by Spielfiedel<sup>19</sup> peak at  $5.7 a_0$ , where the outer well minimum of the  $4^1\Sigma_u^+$  state lies. These were integrated over internuclear separation and weighted by the vibrational wavefunctions of the initial and final states to obtain calculated transition strengths. The experimental results shown in Fig. 8

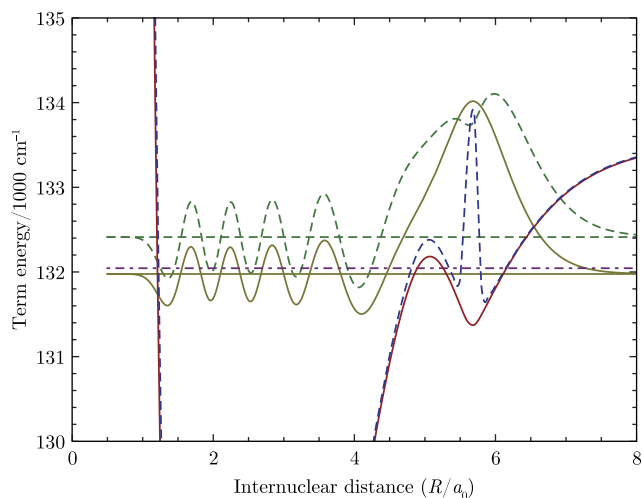


FIG. 7. Comparison of *ab initio* Born-Oppenheimer (solid) and adiabatic (dashed) potential energy curves and  $v = 9$  vibrational wavefunctions of the  $4^1\Sigma_u^+$  state (Ref. 1). The magenta dotted-dashed line indicates the assigned  $J = 0$  energy value from Table I.

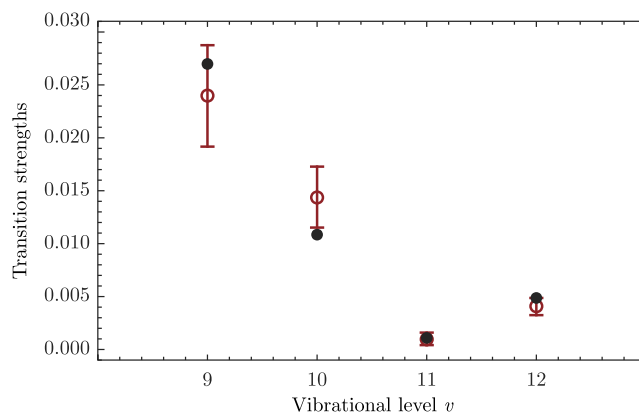


FIG. 8. Calculated (black dots) and measured (red open circles) transition strengths from the  $EF^1\Sigma_g^+$ ,  $v = 6$  state to the  $4^1\Sigma_u^+$ ,  $v$  state.

were determined by integrating P(1) transitions from the spectra to obtain peak areas and have been scaled by an average ratio of the experimental-to-theoretical transition strength. The error bars take into account uncertainty in peak width and the uncertainty due to shot-to-shot variations of the laser intensity. The agreement in the observed trend of transition strength with vibration provides further support for the proposed assignments.

Also shown in Table I are observed linewidths obtained through an analysis of the P(1) and the R(1) probe transitions. These were extracted from the spectra using a Beutler-Fano profile,<sup>23</sup>

$$\sigma(E) = \sigma_0 \frac{(q + \varepsilon)^2}{1 + \varepsilon^2}, \quad (1)$$

where

$$\varepsilon = \frac{2(E - E_0)}{\Gamma}, \quad (2)$$

$q$  is the asymmetry parameter,  $E_0$  is the central energy of the peak, and  $\Gamma$  is the linewidth, which is related to the lifetime  $\tau$  of the state via the relation

$$\tau = \frac{1}{2\pi c \Gamma}. \quad (3)$$

The fits were done at multiple probe laser intensities to extrapolate the zero-intensity linewidth. The probe laser linewidth of  $0.17 \pm 0.02 \text{ cm}^{-1}$  was then deconvolved from this result to obtain the values reported in Table I. The asymmetry parameter,  $q$ , characterizes the relative strength of the transition moments to the discrete and continuum components of the upper level in the transition. As can be seen in the spectra, the peaks are highly symmetric, with  $q$  values typically larger than 10 and with most larger than 15.

There was no significant difference in width as a function of  $J$ , suggesting the decay mechanism involves coupling to a decay channel of  $\Sigma$  character. The relative linewidths indicate substantial coupling of the  $v = 9, 10$ , and  $11$  compared to  $v = 8$  or  $12$ , whose natural widths are on the order of or below the instrument width. A possible candidate for the decay channel is the dissociative, doubly excited ( $2s\sigma$ ,  $2p\sigma$ ) state

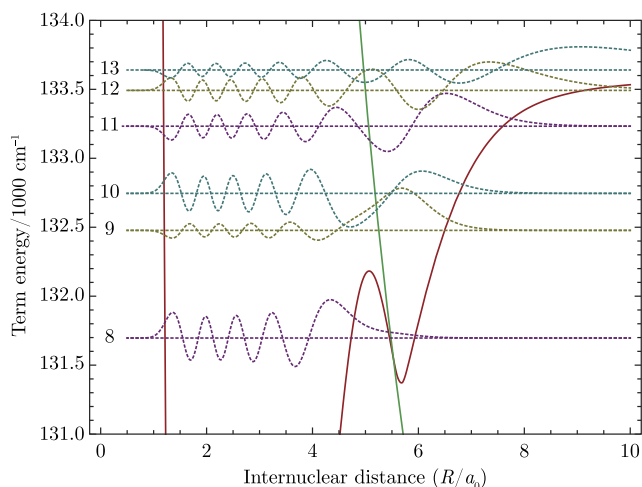


FIG. 9. *Ab initio* potential energy curve (red) and vibrational wavefunctions  $\chi_v(R)$  (dashed) placed at the adiabatic energies<sup>1</sup> of the  $v=8-13$  levels of the  $4^1\Sigma_u^+$  state. The doubly excited ( $2s\sigma$ ,  $2p\sigma$ ) curve<sup>3</sup> (green) is shown to illustrate vibrational wavefunction overlap for  $v \geq 9$ . The curve was extrapolated to  $R > 4$  by using the inner wall of the outer well of the  $B''\bar{B}^1\Sigma_u^+$  state.

which intersects these vibrational wavefunctions of the  $4^1\Sigma_u^+$  state at  $\sim 5 a_0$ .

The decay mechanism can be understood as arising from the crossing of the ( $1s\sigma, 4f\sigma$ ) and the doubly excited ( $2s\sigma$ ,  $2p\sigma$ ) diabatic curves. The bound vibrational wavefunctions of the  $4^1\Sigma_u^+$  state that lie near the crossing acquire dissociative ( $2s\sigma$ ,  $2p\sigma$ ) character and are able to dissociate. In Fig. 9 we compare the location and overlap of the vibrational wavefunctions of the  $v=9-13$  levels of the  $4^1\Sigma_u^+$  state with the continuum region of the doubly excited state. The predominantly inner-well  $v=8$  level has nearly zero vibrational overlap with the continuum region, whereas the  $v \geq 9$  levels have significant overlap leading to measurable but diminishing linewidths as a function of energy. As levels occur further away from the crossing of the two potential energy curves, we expect the coupling to decrease,<sup>24</sup> consistent with the reported linewidths in Table I.

#### IV. CONCLUSIONS

Double-resonance laser spectroscopy via the  $EF^1\Sigma_g^+$ ,  $v'=6$ ,  $J'$  state was used to probe an energy region spanning  $2600 \text{ cm}^{-1}$  below the third dissociation threshold of  $\text{H}_2$ . Assignments of features in the ionization spectra to the  $v=9-12$  levels of the  $4^1\Sigma_u^+$  state are made. Term energies and rotational constants are reported and compared to the theoretical predictions of Staszewska and Wolniewicz.<sup>1</sup> The agreement is reasonable given the strong nonadiabatic mixing expected in this energy region. The measurements have the potential to inform theoretical treatments of nonadiabatic effects in this fundamental molecule. The results also demonstrate the utility of the  $EF^1\Sigma_g^+$  state for investigating high vibrational levels of additional  $f$  states, including the  $4f\pi V^1\Pi_u^+$ ,  $5f\pi V'^1\Pi_u^+$  and  $5f\sigma 6^1\Sigma_u^+$  states,<sup>1,2,25</sup> which could aid in the assignment

of remaining unassigned transitions observed in this energy region.

#### ACKNOWLEDGMENTS

We would like to thank Wenqi Duan, KyungIn Kim, and Zhongying Yan for their assistance with this project. Additionally, we would like to thank Giorgia Corongiu for providing Born-Oppenheimer potential energy curves which aided our assignments.

<sup>1</sup>G. Staszewska and L. Wolniewicz, "Adiabatic energies of excited  $1^1\Sigma_u$  states of the hydrogen molecule," *J. Mol. Spectrosc.* **212**, 208 (2002).

<sup>2</sup>L. Wolniewicz and G. Staszewska, "Excited  $1^1\Pi_u$  states and the  $1^1\Pi_u \rightarrow X^1\Sigma_g^+$  transition moments of the hydrogen molecule," *J. Mol. Spectrosc.* **220**, 45–51 (2003).

<sup>3</sup>I. Sánchez, F. Martín *et al.*, "The doubly-excited states of the  $\text{H}_2$  molecule," *J. Chem. Phys.* **106**, 7720–7730 (1997).

<sup>4</sup>G. Herzberg and Ch. Jungen, "High orbital angular momentum states in  $\text{H}_2$  and  $\text{D}_2$ ," *J. Chem. Phys.* **77**, 5876–5884 (1982).

<sup>5</sup>D. Uy, C. Gabrys, T. Oka, B. Cotterell, R. Stickland, Ch. Jungen, and A. Wüest, "Fine structure of the  $\text{H}_2$   $5g-4f$  inter-Rydberg transition revealed by difference frequency laser spectroscopy," *J. Chem. Phys.* **113**, 10143–10153 (2000).

<sup>6</sup>M. Glass-Maujean, Ch. Jungen, G. Reichardt, A. Balzer, H. Schmoranz, A. Ehresmann, I. Haar, and P. Reiss, "Competing decay-channel fluorescence, dissociation, and ionization in superexcited levels of  $\text{H}_2$ ," *Phys. Rev. A* **82**, 062511 (2010).

<sup>7</sup>Ch. Jungen and M. Glass-Maujean, "Direct optical access to the triplet manifold of states in  $\text{H}_2$ ," *Phys. Rev. A* **93**, 032514 (2016).

<sup>8</sup>D. Bailly, E. J. Salumbides, M. Vervloet, and W. Ubachs, "Accurate level energies in the  $EF^1\Sigma_g^+$ ,  $GK^1\Sigma_g^+$ ,  $H^1\Sigma_g^+$ ,  $B^1\Sigma_u^+$ ,  $C^1\Pi_u$ ,  $B'^1\Sigma_u^+$ ,  $D^1\Pi_u$ ,  $I^1\Pi_g$ ,  $J^1\Delta_g$  states of  $\text{H}_2$ ," *Mol. Phys.* **108**, 827–846 (2010).

<sup>9</sup>G. D. Dickenson, E. J. Salumbides, M. Niu, Ch. Jungen, S. C. Ross, and W. Ubachs, "Precision spectroscopy of high rotational states in  $\text{H}_2$  investigated by doppler-free two-photon laser spectroscopy in the  $EF^1\Sigma_g^+ \leftarrow X^1\Sigma_g^+$  system," *Phys. Rev. A* **86**, 032502 (2012).

<sup>10</sup>L. Wolniewicz, T. Orlikowski, and G. Staszewska, " $1^1\Sigma_u$  and  $1^1\Pi_u$  states of the hydrogen molecule: Nonadiabatic couplings and vibrational levels," *J. Mol. Spectrosc.* **238**, 118–126 (2006).

<sup>11</sup>R. C. Ekey, A. Marks, and E. F. McCormack, "Double resonance spectroscopy of the  $B''\bar{B}^1\Sigma_u^+$  state of  $\text{H}_2$ ," *Phys. Rev. A* **73**, 023412 (2006).

<sup>12</sup>R. C. Ekey, A. E. Cordova, W. Duan, A. M. Chartrand, and E. F. McCormack, "Double resonance spectroscopy of the  $D^1\Pi_u^+$  and  $B''\bar{B}^1\Sigma_u^+$  states near the third dissociation threshold of  $\text{H}_2$ ," *J. Phys. B* **46**, 235101 (2013).

<sup>13</sup>A. M. Chartrand, W. Duan, R. C. Ekey, and E. F. McCormack, "Observations of the high vibrational levels of the  $B''\bar{B}^1\Sigma_u^+$  state of  $\text{H}_2$ ," *J. Chem. Phys.* **144**, 014307 (2016).

<sup>14</sup>M. Glass-Maujean, Ch. Jungen, A. Spielfiedel, H. Schmoranz, I. Tulin, A. Knie, P. Reiss, and A. Ehresmann, "Experimental and theoretical studies of excited states of  $\text{H}_2$  observed in the absorption spectrum: I. The  $5p\pi D''^1\Pi_u$  state," *J. Mol. Spectrosc.* **293-294**, 1–10 (2013).

<sup>15</sup>M. Glass-Maujean, Ch. Jungen, H. Schmoranz, I. Tulin, A. Knie, P. Reiss, and A. Ehresmann, "Experimental and theoretical studies of excited states of  $\text{H}_2$  observed in the absorption spectrum: II. The  $6p\pi$  and  $7p\pi^1\Pi_u$  states," *J. Mol. Spectrosc.* **293-294**, 11–18 (2013).

<sup>16</sup>M. Glass-Maujean, Ch. Jungen, H. Schmoranz, I. Tulin, A. Knie, P. Reiss, and A. Ehresmann, "Experimental and theoretical studies of excited states of  $\text{H}_2$  observed in the absorption spectrum: III. The  $5p\sigma$ ,  $6p\sigma$  and  $7p\sigma$  states," *J. Mol. Spectrosc.* **293-294**, 19–26 (2013).

<sup>17</sup>M. Glass-Maujean, H. Schmoranz, I. Haar, A. Knie, P. Reiss, and A. Ehresmann, "The  $J=1$  para levels of the  $v=0$  to 6 np singlet Rydberg series of molecular hydrogen revisited," *J. Chem. Phys.* **136**, 134301 (2012).

<sup>18</sup>M. Glass-Maujean, H. Schmoranz, I. Haar, A. Knie, P. Reiss, and A. Ehresmann, "The  $J=2$  ortho levels of the  $v=0$  to 6 np singlet Rydberg series of molecular hydrogen revisited," *J. Chem. Phys.* **137**, 084303 (2012).

<sup>19</sup>A. Spielfiedel, "Ab initio calculation of electronic transition moments for singlet excited states of the  $\text{H}_2$  molecule," *J. Mol. Spectrosc.* **217**, 162–172 (2003).



- <sup>20</sup>R. C. Ekey and E. F. McCormack, "Spectroscopic observation of bound ungerade ion-pair states in molecular hydrogen," *Phys. Rev. A* **84**, 020501 (2011).
- <sup>21</sup>M. Glass-Maujean, S. Klumpp, L. Werner, A. Ehresmann, and H. Schmoranz, "The study of the  $D'^1\Pi_u$  state of  $H_2$ : Transition probabilities from the ground state, predissociation yields, and natural linewidths," *J. Chem. Phys.* **128**, 094312 (2008).
- <sup>22</sup>G. D. Dickenson, T. I. Ivanov, M. Roudjane, N. de Oliveira, D. Joyeux, L. Nahon, W.-Ü. L. Tchang-Brillet, M. Glass-Maujean, I. Haar, A. Ehresmann *et al.*, "Synchrotron vacuum ultraviolet radiation studies of the  $D'^1\Pi_u$  state of  $H_2$ ," *J. Chem. Phys.* **133**, 144317 (2010).
- <sup>23</sup>U. Fano, "Effects of configuration interaction on intensities and phase shifts," *Phys. Rev.* **124**, 1866 (1961).
- <sup>24</sup>P. F. Bernath, *Spectra of Atoms and Molecules* (Oxford University Press, 1995).
- <sup>25</sup>G. Corongiu and E. Clementi, "Energy and density analysis on the  $H_2$  molecule from the united atom to dissociation: The  $\Sigma$ ,  $\Pi$ ,  $\Delta$ ,  $\Phi$ , and  $\Gamma$  manifolds," *Int. J. Quantum Chem.* **111**, 3517–3540 (2011).